

# SIMULATION OF FLOW IN A RADIAL FLOW FIXED BED REACTOR (RFBR)

Aqeel A. KAREERI, Habib H. ZUGHBI\*, and Habib H. AL-ALI\*

Ras Tanura Refinery, SAUDI ARAMCO, Saudi Arabia  
\*Department of Chemical Engineering,  
King Fahd University of Petroleum & Minerals KFUPM,  
Dhahran, Saudi Arabia  
Email: [aqeel.kreeri@aramco.com.sa](mailto:aqeel.kreeri@aramco.com.sa)

## ABSTRACT

The flow in a radial flow fixed bed reactor (RFBR) was simulated using computational fluid dynamics (CFD). There are four types of RFBR based on the axial direction of the flow in the distributing channel and the center pipe and the reactor radial flow direction. These types are known as CP-z, CP- $\pi$ , CF-z and CF- $\pi$  configurations. Flow in all four configurations was simulated. The model results showed good agreement with published experimental data. Results also showed that one of the  $\pi$ -flow configurations has always the most uniform axial flow compared to the z-flow configurations under the same conditions. Results also showed that if the ratio of the cross sectional area of the center pipe to that of the annular channel is less than one, the CF- $\pi$  configuration gives the best uniform flow. For an area ratio larger than one, the CP- $\pi$  configuration gives the best uniform flow.

**Key words:** Radial flow reactors, computational fluid dynamics, fixed bed, flow distribution.

## NOMENCLATURE

$A_f$	perforated plate holes total area, m <sup>2</sup>
$A_p$	perforated plate total area, m <sup>2</sup>
C	orifice discharge coefficient
$C_2$	inertial resistance factor, 1/m
$D_p$	catalyst particle diameter, m
g	acceleration due to gravity, 9.81 m/s <sup>2</sup>
P	pressure, Pa
S	source term, Pa/m
t	perforated plate thickness, m
v	velocity, m/s
$\rho$	density, kg/m <sup>3</sup>
$\epsilon$	packing void
$\alpha$	Permeability resistance factor, m <sup>2</sup>
$\mu$	viscosity, Pa s

## INTRODUCTION

A radial reactor is a cylindrical vessel with especially designed internals. Figure 1 shows the main internals in a radial flow fixed bed reactor (RFBR). The main internals that provide the radial flow pattern inside the reactor are the inlet distributing header in the form of perforated channels positioned around the

circumference of the vessel, and the axial outlet collecting header in the form of a perforated cylinder which is called the center pipe. The catalyst is charged to the annular space between the inlet distributor and the center pipe. The top of the catalyst bed is covered with a cover plate. There are two types of inlet distributors. One consists of a wire screen while the other consists of a series of scallops (Little, 1985), where each scallop is a small diameter perforated half cylinder.

Radial flow reactors can be classified into a z-flow type or a  $\pi$ -flow type depending on the axial direction of the flow in the distributing channel and the center pipe. Moreover, radial flow reactors can be also classified into centripetal (CP) or centrifugal (CF) flow types depending on the reactor radial flow direction. In the CP-flow type, the gas is fed to the distributing channel and travels radially from the outer screen to the center pipe. In the CF-flow configuration the gas is fed to the center pipe and travels radially from the center pipe to the outer screen. Therefore, four flow configurations are possible for a radial flow reactor. They are classified as CP-z, CP- $\pi$ , CF-z and CF- $\pi$  configurations as shown in Figure 2.

The RFBR was originally used in the catalytic synthesis of ammonia. Subsequently it was used for catalytic reforming, desulphurization, and nitric oxide conversion. Earlier analytical work on an RFBR concentrated on the effects of radial flow direction on reaction conversion with the assumption of perfect radial flow profile inside the reactor (Chang and Calo, 1981). Ponzi and Kaye (1979) were the first to show that flow maldistribution inside the RFBR has more influence on the reactor performance than the flow direction. Heggs *et al.* (1994) performed a numerical investigation for all four configurations. The ratio of the cross-sectional area of the center pipe to that of the annular channel was greater than one. It was concluded that the CP- $\pi$  flow configuration gives the best flow distribution. Heggs *et al.* (1995) extended their previous model to predict the flow profiles for a multi-layered radial flow air filter. A good agreement was found between model predictions and experimental results. Heggs *et al.* (1994,1995) numerical work was based on a simplified one-dimensional momentum balance. Mu *et al.* (2003) also investigated the flow in a radial flow reactor using a modified two-dimensional momentum equation which required an empirically determined term. This term

could not be easily determined for industrial reactors. A survey of the literature shows that no rigorous three-dimensional computational fluid dynamics simulation of flow in a radial flow fixed bed reactor has been carried out. Three-dimensional simulations are important because they show the effects of the change in the flow area in the radial direction. Two-dimensional simulations assume a constant flow area.

From the previous work, it is shown that the flow distribution has a major effect on the operations of an RFBR. The objective of this work is to use computational fluid dynamic (CFD) to study the flow distribution in an RFBR.

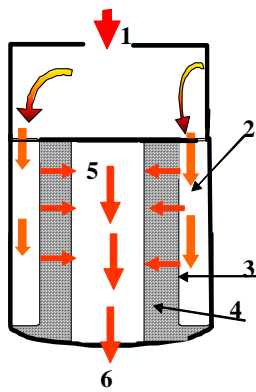


**Figure 1:** A schematic diagram of an RFBR, (1) reactor inlet, (2) annular channel, (3) inlet distributor, (4) catalyst bed, (5) center pipe, and (6) reactor outlet.

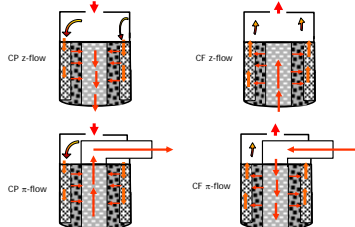


**Figure 2:** The four possible flow configurations for an RFBR.

### FLOW DISTRIBUTION IN AN RFBR

The operating efficiency of a radial flow reactor largely depends on the gas stream distribution over the catalyst bed height. Figure 3 shows typical flow distributions in a radial flow reactor. To have a uniform flow distribution, the gas mass flow should be equally divided over the catalyst bed height. If the mass flow is not equally divided some parts of the bed will be under-utilized as found by Lobanov and Skipin (1986). A non-uniform flow distribution over the bed height affects the reaction conversion and selectivity and the temperature profile (Ponzi and Kaye, 1979; Lobanov and Skipin, 1986; Suter *et al.*, 1990).

Having an optimum or a poor utilization of the catalyst bed depends mainly on the pressure distribution inside the reactors. An important design criterion for the radial flow reactor is to have the radial pressure independent of the axial coordinate (Chang *et al.*, 1983). This criterion makes the gas stream equally divided over the catalyst volume as shown in Figure 3a for CP configurations and in Figure 3d for CF configurations. In other words, the uniformity criterion means achieving a uniform flow distribution in a radial flow reactor by having the pressure drop be the same, at any axial level, between the center pipe and the annular channel.

In the present study, the conservation equations of mass and momentum in conjunction with porous media and porous jump models are used to describe

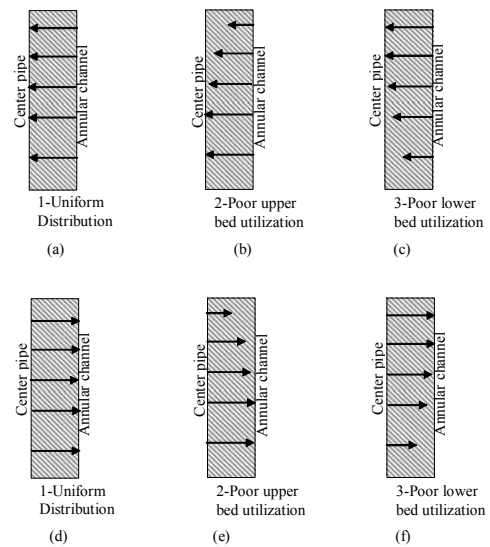


**Figure 3:** Typical flow distributions over the bed length in a radial flow reactor at the same feed flow rate for CP configurations (a-c) and for CF configurations (d-f). The arrow length represents the mass flow magnitude.

the flow in an RFBR. In addition, a three-dimensional geometry is used to take into account the effects of the reduction in cross-sectional flow area toward the center pipe. The equations were solved using a general purpose three-dimensional CFD package, Fluent 6.1™.

### THE GOVERNING EQUATIONS

The flow in an RFBR reactor is classified as a single phase flow. The simulation of an RFBR is carried out under no reaction, isothermal, incompressible and steady state conditions. The governing equations for the gas flow in an RFBR are the mass and momentum conservation equations.

The mass conservation equation is:

$$\nabla \cdot \vec{v} = 0 \quad (1)$$

The general form of the momentum conservation equation is:

$$\rho(\vec{v} \cdot \nabla \vec{v}) = -\nabla P + \mu \nabla^2 \vec{v} + \rho \vec{g} + \vec{S} \quad (2)$$

where  $S$  contains other model-dependent source terms. In the present study, two other models are used, these are a porous-media and a porous-jump model. The porous-media model is used for the catalyst bed and the porous-jump model is used for the center pipe and annular perforated plates.

At the catalyst bed:

$$\vec{S} = -\left(\frac{\mu}{\alpha} \vec{v} + C_2 \frac{1}{2} \rho |\vec{v}| \vec{v}\right) \quad (3)$$

where  $\alpha$  is the permeability and  $C_2$  is the inertial resistance factor. From the Ergun equation, which is a semi-empirical correlation applicable over a wide range of Reynolds numbers and for many types of packing,  $\alpha$  and  $C_2$  can be represented by:

$$\alpha = \frac{D_p^2}{150} \frac{\varepsilon^3}{(1-\varepsilon)^2} \quad (4)$$

$$C_2 = \frac{3.5}{D_p} \frac{(1-\varepsilon)}{\varepsilon^3} \quad (5)$$

where  $\varepsilon$  is the bed porosity and  $D_p$  is the catalyst diameter. In this model the bed porosity and catalyst diameter are assumed to be 0.35 and 1.8 mm respectively.

The porous-jump is a simplification of the porous media model where the flow is assumed to be one dimensional, normal to the porous section of the plate. Since the velocity is high through the perforated plate the inertial term is the dominating one. Neglecting the permeability term, the source term at the center pipe and annular perforated plates becomes:

$$\vec{S}_i = -\left(C_2 \frac{1}{2} \rho |\vec{v}| \vec{v}_i\right) \quad (6)$$

where  $i$  is the normal coordinate ( $x$ ,  $y$  or  $z$ ) to the perforated plate.  $C_2$  for the perforated plate is determined from the equation of the flow through square-edged holes on an equilateral triangular spacing.

$$C_2 = \frac{1}{C^2} \frac{(A_p / A_f)^2 - 1}{t} \quad (7)$$

where  $C$  is the orifice discharge coefficient. In this work  $C$  is 0.62. This value is generally used for most of the perforated plates (Perry and Green, 1997).  $A_p$  is the total area of the plate,  $A_f$  is free area or total area of the holes and  $t$  is the plate thickness.

## SIMULATION OF AN RFBR

A schematic diagram of the radial flow reactor simulated in the present study is shown in Figure 4. The reactor consists of two perforated cylinders and a reactor wall. The gas stream enters the annular channel where it is distributed through the perforated plate. It then flows radially across the particle bed towards the center pipe. The driving force of the flow across the bed is the radial pressure drop between the annular channel and the center pipe.

The reactor dimensions and operating conditions used in this study are shown in Tables 1 and 2. Figure 4 represents the conventional configuration, which is the CP-z configuration. The flow in the other three configurations was also simulated.

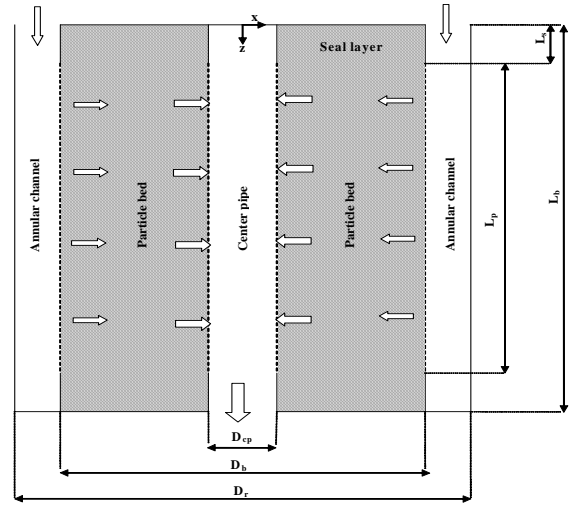


**Figure 4:** A Schematic diagram of a radial flow reactor, where  $L_s$ ,  $L_p$  and  $L_b$  are the lengths of the seal layer, the perforation section and the bed, respectively,  $D_{cp}$  and  $D_r$  are the diameters of the center pipe and the reactor, respectively and  $D_b$  is the outer bed diameter.

A three dimensional numerical model is constructed using the information in Figure 4 and Table 1. The full geometry of the reactor is simulated. No symmetry is used to reduce the computational domain. The geometry is meshed using an unstructured tetrahedral mesh. After checking the grid independency, a mesh size of 18 mm was used and the total number of cells obtained is 535573 cells.

## Simulation Results

In discussing the results, many cuts are made along the height of the center pipe, the annular channel or across the width of the fixed bed. The coordinates where these cuts are taken are shown in Figure 5. Figure 5 shows the values of  $x$  and  $z$  at which cuts are taken and are frequently referred to while discussing the results in the next few sections.

Dimension*	$L_s$	$L_p$	$L_b$	$D_{cp}$	$D_b$	$D_r$
Value (mm)	160	1680	2000	130	410	500

**Table 1:** The reactor dimensions. \*see Figure 4

Boundary Condition	Inlet flow rate (m <sup>3</sup> /h)	Bed porosity	Center pipe porosity	Annular channel Porosity
Value	200	0.35	0.05	0.3

**Table 2:** The boundary conditions used in the present simulations

### Flow Distribution in CP-z and CP- $\pi$ Configurations

Figure 6 shows the axial static pressure in the annular channel and center pipe for the CP-z and CP- $\pi$  configurations. The pressure in the annular channel is almost constant. In the center pipe a higher pressure drop occurs. This high pressure drop affects the flow distribution inside the reactor. In the CP-z the pressure difference between the annular channel and the center pipe is very high at the bottom of the bed, therefore the mass flow will be higher at the bottom which leads

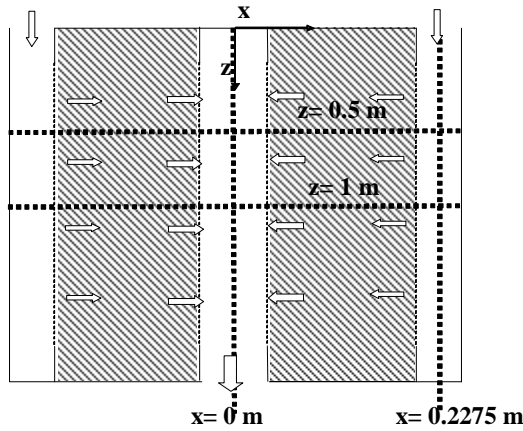


**Figure 5:** A schematic diagram of various values of  $x$  and  $z$  where cuts are taken in subsequent figures. Since the model is symmetric at  $y$ -plane = 0, all cuts are at  $y$ -plane = 0.  $x=0$  and  $x=0.2275$  lines represent the axial flow profiles in the center pipe and the annular channel respectively.  $z=0.5$  and  $z=1$  lines represent the radial flow profiles in the reactor.

to a poor utilization of the upper part of the bed. In the CP- $\pi$  configuration there will be a poor utilization of the bottom part of the bed. The flow distributions for the CP-z and CP- $\pi$  configurations are the same as those shown in Figure 3b and 3c respectively. To improve the flow distribution, the pressure drop in the

center pipe should be lowered and this can be done by increasing its diameter.

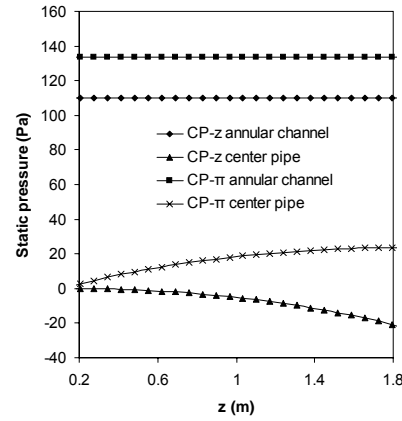


**Figure 6:** The axial static pressure profile in the annular channel and the center pipe of a CP-z and a CP- $\pi$  configurations.

### Flow Distribution in CF-z and CF- $\pi$ Configurations

Figure 7 shows the axial static pressure in the annular channel and the center pipe for the CF-z and CF- $\pi$  configurations. In the CF configurations, the center pipe is the discharge channel and the annular channel is the collecting channel. A significant pressure rise occurs in the center pipe. The pressure difference between the annulus and the center pipe is higher at the reactor bottom. The flow distribution for the CF-z and CF- $\pi$  configurations is the same as that shown in Figure 3e. Despite of that the annulus and the center pipe pressure profiles are closer to a parallel profile than that for CP configurations.

### Uniformity Analysis for the Four Configurations

From the previous results, it was seen that each configuration of the radial flow reactor gives a different flow profile. In this analysis, the uniformity criterion of Chang *et al.* (1983) is used. In a uniform

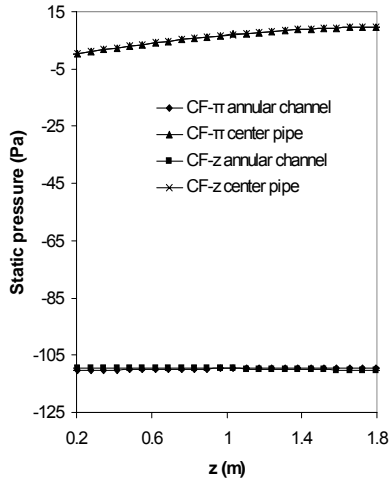


**Figure 7:** The axial static pressure profile in the annular channels and the center pipes of CF-z and CF- $\pi$  configurations.

flow distribution, the pressure drop between the annular channel and center pipe is the same along the bed height. Figure 8 shows the radial pressure drop along the bed height for the four configurations. Figure 8 also shows that the CP-z and CP- $\pi$  configurations have a higher reactor pressure drop than CF-z and CF- $\pi$  configurations. This indicates that a flow maldistribution contributes to the reactor pressure drop.

In all four configurations, the radial pressure drop profile shows dependency on the axial position, which is a deviation from uniformity. To have one base for the four configurations for comparisons, the radial pressure drop profile for each configuration was normalized by dividing it by the maximum radial pressure drop.

Figure 9 shows the deviation of each configuration from the uniform flow. The normalized radial pressure drop for the uniform flow equals one at any axial position. From this figure it seems that CF- $\pi$  configuration is the best configuration which is the closest to the uniform line. The second best is the CF-z. CP-z and CP- $\pi$  show almost the same deviation from the uniformity. They have the lowest flow uniformity.

#### **Validation against the Data of Heggs *et al.*, (1995)**

A CFD model is constructed to simulate the radial flow in a multi-layered air filter used by Heggs *et al.* (1995). A schematic diagram of the model of Heggs *et al.* (1995) is shown in Figure 10. It is a CF-z configuration. The present CFD model is used to simulate an RFBR identical to that used by Heggs *et al.* (1995) with the same flow and boundary conditions. Three flow rates of 85, 152 and 255 m<sup>3</sup>/h

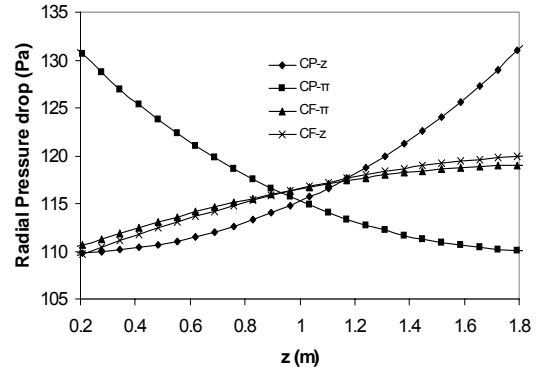


**Figure 8:** Radial pressure drop variation along the perforated section length.

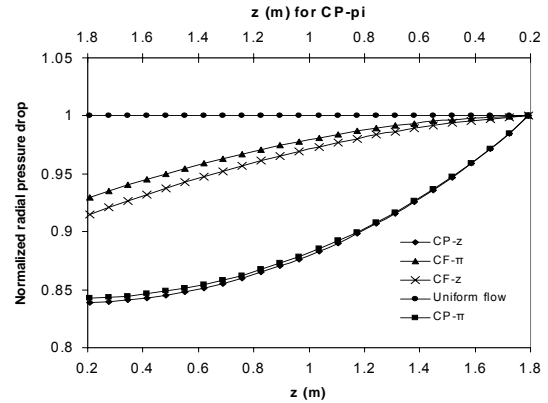


**Figure 9:** Deviation from uniform flow for the four radial flow configurations.

are used. Table 3 shows a comparison of the experimental and numerical results of Heggs *et al.* (1995) and the present CFD simulation results.

Heggs *et al.* (1995) also compared their measurements with predictions of the pressure profiles in the center pipe and the annular channel. The pressure profile for the center pipe was normalized by dividing it by the maximum pressure rise and the pressure profile of the annular channel was normalized by dividing it by the maximum pressure fall. Figures 11 and 12 show a comparison of the present study normalized pressure profiles of the center pipe and the annular channel respectively with those of Heggs *et al.* (1995).

It can be seen from Table 3 and Figures 11 and 12 that the CFD model shows a good agreement with experimental measurements. Furthermore, the CFD results are closer to the experimental results than the numerical predictions of Heggs *et al.* (1995). This is because Heggs *et al.* (1995) did not include the small

inlet pipe above the center pipe that is shown in Figure 10. The inlet pipe above the center pipe has a smaller cross sectional area, which causes the flow to enter the center pipe as a high velocity jet. This causes a sharp pressure rise at the top section of the center pipe since a high velocity is maintained there and there is almost no flow reduction in the radial direction. Heggs *et al.* (1995) also mentioned that there are other flow obstructions at the inlet of the center pipe. There are no details about these obstructions. Implementing those details is likely to make the CFD results even closer to the experimental measurements. Despite of that, the model gives good prediction for such a complex flow in a multi-layered radial flow filter. An advantage shown by the model is that it can include any external piping that may affect the flow profile in the radial flow reactor.

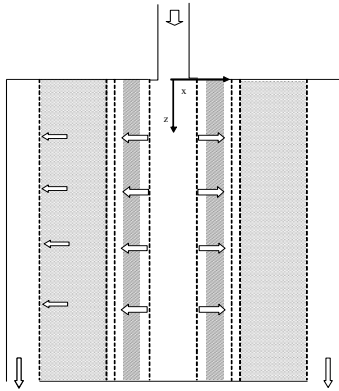


**Figure 10:** A schematic diagram of the multi-layered radial flow air filter used by Heggs *et al.* (1995).

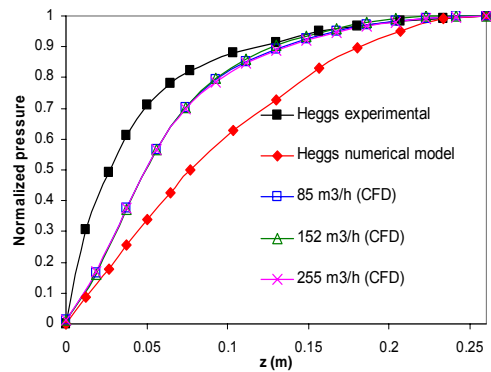


**Figure 11:** The profile of normalized pressure in the center pipe.

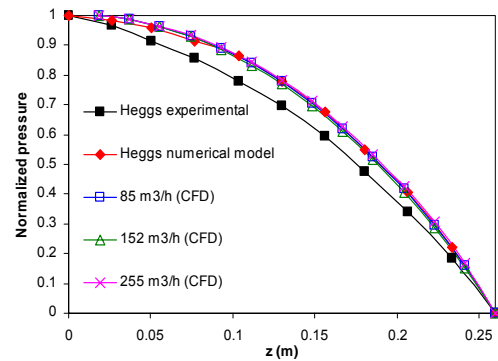


**Figure 12:** The profile of normalized pressure in the annular channel.

Flow rate (m <sup>3</sup> /h)	Measurement and prediction	Pressure rise in center pipe (Pa)	Pressure fall in annular channel (Pa)	Total pressure drop (Pa)
85	Heggs experimental	5.1	48.1	362.5
	Heggs numerical	2.0	16.5	380.7
	CFD simulation results	5.3	31.9	345
152	Heggs experimental	16.0	142.9	748
	Heggs numerical	6.4	53.7	748.6
	CFD simulation results	16.6	97.6	710
255	Heggs experimental	41.3	349.2	1400
	Heggs numerical	17.9	146.0	1315
	CFD simulation results	45.8	266.8	1428

**Table 3:** Heggs *et al.* (1995) pressure measurement and prediction at different flow rates.

### Effects of the Ratio of the Center Pipe to the Annular Channel Cross Sectional Area

The effects of the ratio of the center pipe to the annular channel cross sectional area were investigated numerically and experimental for the CF- $\pi$  configuration by Genkin *et al.* (1973). It was found that increasing this ratio will improve the flow distribution in a CF- $\pi$  configuration. Chang and Calo (1981) found that at a ratio of 1,  $\pi$ -flow configurations will have the most uniform flow distribution. Mu *et al.* (2003) found that there is an optimum ratio at which the CP- $\pi$  configuration has the most uniform flow distribution. In the present work, the effects of this ratio for all four radial flow configurations were investigated. Figure 9 and Table 4 shows that CF- $\pi$  configuration has the best flow distribution at a ratio of 0.21 (less than one). When this ratio is increased to one, a more uniform flow distribution was achieved by all configurations. Increasing the ratio was done by increasing the center pipe cross sectional area. The annular channel and bed cross sectional areas and the reactor height were kept the same as those in Table 1. At a ratio of one,  $\pi$ -flow configurations have the most uniform flow distribution as shown in Table 4. At a ratio of 1.8 (greater than one), a CP- $\pi$  configuration has the best flow distribution. It seems that both or one of the  $\pi$ -flow configurations will always have the most uniform flow distribution.

The sign of the non-uniformity values for the CF- $\pi$  and the CP- $\pi$  configurations change as the ratio increases. This change of the sign of the non-uniformity indicates that an optimum value is passed. The optimum ratio for CF- $\pi$  configuration is between 0.21 and 1 and that for CP- $\pi$  is between 1 and 1.8. A high ratio produces a low reactor pressure drop and hence a low reactor operating cost. Therefore the CP- $\pi$  configuration is the superior configuration for the radial flow reactor.

### CONCLUSIONS

Flow in a radial flow fixed bed reactor (RFBR) is simulated using computational fluid dynamics. All four RFBR flow configurations, namely CP-z, CP- $\pi$ , CF-z and CF- $\pi$ , were investigated. When the ratio of the center pipe cross sectional area to the annular channel cross sectional area is less than one the CF- $\pi$  configuration was found to have the lowest flow maldistribution. A reactor with a uniform flow has lower pressure drop than a reactor with a flow maldistribution.

The numerical model was quantitatively validated against the published results of Hegggs *et al.* (1995) and the CFD simulation results were in good agreement with the experimental results.

The ratio of the center pipe to the annular channel cross sectional area has a major impact on the reactor uniformity. At a ratio less than one, CF-flow configurations show the best flow distribution and the CF- $\pi$  configuration produces the most uniform flow distribution. At a ratio of one, both  $\pi$ -flow configurations produce the most uniform flow distribution. At a ratio larger than one, CP-flow configurations show the best flow distribution and the CP- $\pi$  configuration produces the most uniform flow distribution. It was shown that one of the  $\pi$ -flow types always has the most uniform flow distribution. From an energy saving point of view, the CP- $\pi$  configuration is the best configuration for a radial flow reactor since it can have uniform flow distribution at a low reactor pressure drop. RFBR should be designed at the optimum ratio that will produce the most uniform flow distribution.

Radial flow configuration	non-uniformity		
	Ratio(0.21)<1	Ratio=1	Ratio(1.8)>1
CP-z	0.084	0.013	0.010
CP- $\pi$	-0.089	-0.006	0.001
CF- $\pi$	0.036	-0.006	-0.013
CF-z	0.044	0.014	0.017

**Table 4:** Non-uniformities at different ratios cross sectional areas

$$\text{where } non - uniformity = 1 - \sqrt{\frac{Radial \Delta P_{entrance}}{Radial \Delta P_{closed end}}} \quad (\text{Song } et al., 1993)$$

### Acknowledgement

The authors would like to acknowledge the support of KFUPM and ARAMCO Company during the course of this work and the preparation of this paper.

### REFERENCES

CHANG H. C.; SAUCIER, M.; CALO, J. M.,(1983), "Design Criterion for Radial Flow Fixed-Bed Reactors.", *AIChE J.*, **29**, 1039.

CHANG, H. C.; CALO, J. M., (1981), "An Analysis of Radial Flow Packed Bed Reactors-How Are They Different.", *ACS Symp. Ser.*, **168**, 305.

ERGUN, S., (1952) "Fluid Flow through Packed Columns.", *Chem. Eng. Prog.*, **48**, 89.

FLUENT 6.1 Manual, (1998), Fluent Inc., Lebanon, NH USA.

GENKIN, V. S.; DIL'MAN, V. V.; SERGEEV, S. P., (1973), "The Distribution of a Gas Stream Over a Radial Contact Apparatus.", *Int. Chem. Eng.*, **13**, 24.

HEGGS, P. J.; ELLIS, D. I.; ISMAIL, M. S., (1994), "The Modeling of Fluid-Flow Distributions in annular Packed Beds.", *Gas Sep. & Pur.*, **8**, 257.

HEGGS, P. J.; ELLIS, D. I.; ISMAIL, M. S., (1995), "Prediction of Flow Distributions and Pressure Changes in Multi-Layered Annular Packed Beds.", *Gas Sep. & Pur.*, **9**, 243.

LITTLE, D. M., (1985) Catalytic Reforming, PennWell, Tulsa, OK.

LOBANOV, E. L.; SKIPIN, Y. A., (1986), "Increasing the Operating Efficiency of Radial Reactors in Reforming.", *Chem. Tech. Fuels Oil*, **22**, 275.

MU, Z.; WANG, J.; WANG, T.; JIN, Y., (2003), "Optimum Design of Radial Flow Moving-Bed Reactors Based on a Mathematical Hydrodynamic Model.", *Chem. Eng. & Process.*, **42**, 409.

PERRY, R. H.; GREEN, D., (1997), Chemical Engineer's Handbook **7<sup>th</sup> edn**, McGraw-Hill, Section 6, New York, USA.

PONZI, P. R.; KAYE, L. A., (1979), "Effects of Flow Maldistribution on Conversion and Selectivity in Radial Flow Fixed-Bed Reactors.", *AIChE J.*, **25**, 100.

SONG, X.; WANG, Z.; JIN, Y.; GONG, M., (1993), "Investigations on Hydrodynamics of Radial Flow Moving Bed Reactors.", *Chem. Eng. Technol.*, **16**, 383.

SUTER, D.; BARTROLI, A.; SCHNEIDER, F.; RIPPIN, D. W. T.; NEWSON, E. J., (1990), "Radial Flow Reactor Optimization for Highly Exothermic Selective Oxidation Reactions.", *Chem. Eng. Sci.*, **45**, 2169.